Article No. jmbi.1999.2875 available online at http://www.idealibrary.com on IDEAL® J. Mol. Biol. (1999) 290, 229–240

JMB

Domain Motions Accompanying Tet Repressor Induction Defined by Changes of Interspin Distances at Selectively Labeled Sites

Beatrix Tiebel[1], Nicole Radzwill[2], Lwin Mar Aung-Hilbrich[1], Vera Helbl[1] Heinz-Jürgen Steinhoff[2] and Wolfgang Hillen[1]*

[1]*Lehrstuhl für Mikrobiologie Biochemie und Genetik der Friedrich-Alexander Universität Erlangen-Nürnberg Staudtstrasse 5 91058, Erlangen, FRG*

[2]*Lehrstuhl für Biophysik der Ruhr-Universität Bochum Universitätsstrasse 150 44780, Bochum, FRG*

**Corresponding author*

To investigate internal movements in Tet repressor (TetR) during induction by tetracycline (tc) we determined the interspin distances between pairs of nitroxide spin labels attached to specific sites by electron paramagnetic resonance (EPR) spectroscopy. For this purpose, we constructed six TetR variants with engineered cysteine pairs located in regions with presumed conformational changes. These are I22C and N47C in the DNA reading head, T152C/Q175C, A161C/Q175C and R128C/D180C near the tc-binding pocket, and T202C in the dimerization surface. All TetR mutants show wild-type activities *in vivo* and *in vitro*. The binding of tc results in a considerable decrease of the distance between the nitroxide groups attached to both I22C residues in the TetR dimer and an increase of the distance between the N47C residues. These opposite effects are consistent with a twisting motion of the DNA reading heads. Changes of the spin-spin interactions between nitroxide groups attached to residues near the tc-binding pocket demonstrate that the C-terminal end of α-helix 9 moves away from the protein core upon DNA binding. Alterations of the dipolar interaction between nitroxide groups at T202C indicate different conformations for tc and DNA-bound repressor also in the dimerization area. These results are used to model structural changes of TetR upon induction.

Keywords: tetracycline; electron spin resonance spectroscopy; spin labels; dipolar interaction; site-directed spin-labeling

Introduction

Alternative structures of proteins and their dynamics play crucial roles in the control of many biological processes. Structural changes observed in bacteriorhodopsin during the photocycle show that protein movements are important in energy metabolism (e.g. for a review, see Oesterhelt, 1998), and receptor proteins often make use of defined conformational changes to transmit information as part of a signal transduction chain (Careaga & Falke, 1992; Lee *et al.*, 1995). Many proteins active in regulation of transcription are triggered by effectors to switch between DNA-binding and non-binding states. The conformational changes underlying these different activities are the mechanistic basis of gene regulation. They have been postulated for many bacterial regulatory proteins, but detailed information about the nature and magnitude of these motions is rare. There is presently no common pattern of structural changes resulting in altered DNA binding. Catabolite responsive protein CRP and the tryptophan repressor TrpR belong to a group of regulatory proteins where effector binding leads to another orientation of the DNA-binding domains with respect to the ligand-binding domains (Zhang, *et al.*, 1987; Kolb *et al.*, 1993), whereas parts of the protein core are involved in structural changes in Lac repressor (Lewis *et al.*, 1996). No structural changes at all were found in the methionine repressor MetJ (Cooper *et al.*, 1994).

Abbreviations used: EPR, electron paramagnetic resonance; tc, tetracycline; CRP, catabolite responsive protein; HTH, α-helix-turn-α-helix; SDSL, site-directed spin-labeling; MTS, (1-oxyl-2,2,5,5-tetramethylpyrroline-3-methyl) methane thiosulfonate.

E-mail address of the corresponding author: whillen@biologie.uni-erlangen.de

0022-2836/99/260229–12 $30.00/0

We have studied the importance of dynamics for the tetracycline (tc)-inducible Tet repressor TetR (Beck *et al.*, 1982; Hillen & Berens, 1994; Gossen *et al.*, 1995). The crystal structures of the inducer-free TetR and the TetR-($[Mg\text{-}tc]^+$)$_2$-complex (Hinrichs *et al.*, 1994; Kisker *et al.*, 1995; Orth *et al.*, 1998) and the characterization of non-inducible TetR mutants (Hecht *et al.*, 1993; Müller *et al.*, 1995) have suggested conformational changes of TetR upon tc binding. The DNA-recognition helices in the induced TetR dimer are 3.9 nm apart and tilted by 110° with respect to each other, rendering it unable to bind to successive major grooves of *B*-type DNA. Fluorescence quenching studies have indeed indicated a movement of the α-helix-turn-α-helix motif (HTH) during induction (Hansen *et al.*, 1987). The redox-dependent activity of TetR variants with suitably located cysteine residues has also confirmed that several movements are necessary for induction (Tiebel *et al.*, 1998). However, no data presently available directly address the detailed nature and scale of these movements.

We used site-directed spin-labeling (SDSL) to study the conformational changes of TetR in solution as in previous studies, e.g. with rhodopsin (Farrens *et al.*, 1996), lysozyme (Mchaourab *et al.*, 1997), insulin (Steinhoff *et al.*, 1997) and a potassium channel (Perozo *et al.*, 1998). For this purpose, we have introduced spin labels at selected positions using cysteine substitution mutagenesis followed by modification of the sulfhydryl group with a nitroxide reagent (Hubbell & Altenbach, 1994; Hubbell *et al.*, 1996). The dynamics of the spin labels together with structural information of the protein allow the elucidation of conformational changes in space and time on a millisecond time-scale (Steinhoff *et al.*, 1994, 1995). The estimation of interspin distances in the different complexes of TetR defines regions undergoing structural changes and yields detailed information about the scale of these internal movements (Steinhoff *et al.*, 1997).

Results and Discussion

Sites for spin-labeled cysteine residues

Conformational changes in TetR proposed from crystallographic and genetic analyses have led to two models (Hinrichs *et al.*, 1994; Müller *et al.*, 1995) for the transition from the DNA-bound to the tc-bound state of TetR. The latter is shown in Figure 1. In the first model, a movement of α-helix 4 connecting the DNA reading head with the protein core adjusts the distance between the two DNA reading heads (Hinrichs *et al.*, 1994; Kisker *et al.*, 1995). Mutations located in the contacting area between the DNA reading head and the protein core render TetR non-inducible, supporting such movements, but many more of them are located at the dimer interface and are not explained by this model. Thus, the second induction model (Müller *et al.*, 1995) assumes a tc-induced reorientation of the four-helix bundle formed by α8 and α10 of both monomers. This would require a relocation of α9

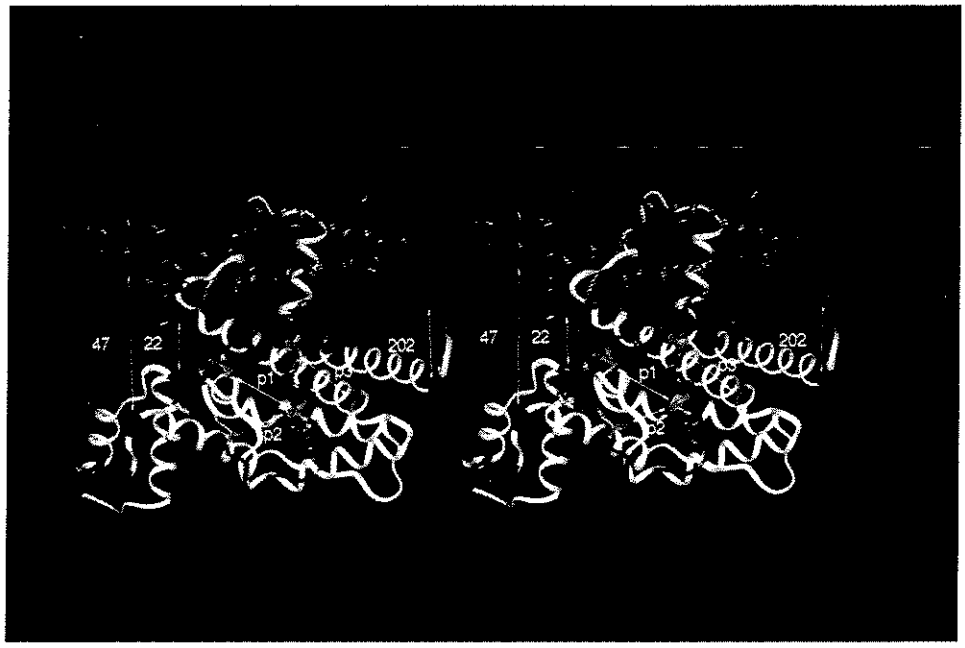

Figure 1. Stereo view of the crystal structure of TetR-($[Mg\text{-}tc]^+$)$_2$ with indicated locations of engineered cysteine residues. The two monomers of TetR are shown as yellow and gray ribbons, respectively; tc is shown as a green stick model and the recognition helices α3 and α3′ of the two HTH are colored in red. The cysteine exchanges I22C and N47C (both in red) and N18C (orange) are located in the DNA reading head. The blue colored cysteine pairs p1 (T152C/Q175C), p2 (A161C/Q175C) and p3 (R128C′/D180C) are located around the tc-binding pocket and indicated in the yellow monomer only. The cysteine exchange T202C (green) is localized in the C-terminal α-helix 10. The arrows connect cysteine pairs that were modified with spin labels to determine interspin distances.

which packs against the four-helix bundle in the induced conformation.

The quantitative analysis of the absolute internitroxide distances at sites expected to move upon induction as suggested by these models is aimed at characterizing those conformational changes. Since the quantitative analysis requires interspin distances of less than ~2.0 nm, we searched the crystal structure of TetR-([Mg-tc]$^+$)$_2$ (Hinrichs *et al.*, 1994; Kisker *et al.*, 1995) for pairs of amino acid residues with the appropriate distances located in regions where we assume movements. We mutated six pairs of amino acids to cysteine in TetR(D), which does not contain an endogenous cysteine residue. These are depicted in the crystal structure of TetR in Figure 1. The distances between spin labels at the cysteine pairs I22C/I22C′ and N47C/N47C′ (a prime notes residues from the second monomer) should define movements of the DNA reading heads with respect to each other. Spin labels bound at cysteine residues T202C and T202C′ should detect movements in the C-terminal α-helix 10 of TetR, reflecting a rearrangement of the dimerization surface as proposed in the second induction model. The cysteine pairs T152C/Q175C (p1), A161C/Q175C (p2) and R128C′/D180C (p3) are designed to detect movements of α-helix 9 and the adjacent loop between α8 and α9 (see p1 - p3 in Figure 1). The respective TetR dimers contain two pairs of cysteine residues that are more than 3.5 nm apart. Spin labels attached to the residues on opposite sides of the dimer show no detectable interaction and hence do not influence this analysis. The distances between the C$^\beta$ atoms of all cysteine pairs based on the induced form of TetR are presented in Table 1.

Functional characterization of the TetR mutants

To determine *in vivo* repression efficiencies the *tetR* variants located on pWH624 were transformed into *Escherichia coli* WH207 pWH1012, where they are constitutively expressed (Berens *et al.*, 1997). The expression of the *tetA-lacZ* transcriptional fusion located on the plasmid pWH1012 was determined at 28 °C in the presence and absence of 0.4 μM tetracycline (tc). The results are shown in Table 2. All *tetR* mutants and wild-type lead to identical repression and induction efficiencies in this assay. These results establish that the cysteine mutations do not affect the activities of the TetR variants *in vivo*. Thus, they are valid probes for physical analysis of their conformational changes.

The mutant TetR proteins were purified to homogeneity and quantitatively modified using (1-oxyl-2,2,5,5-tetramethylpyrroline-3-methyl) methanethiosulfonate (MTS) to place the nitroxide probes onto the cysteine side-chains. The yield was greater than 80 %, except for N47C and T202C, which formed disulfide bonds and showed labeling yields around 40 %. *In vitro* operator binding of the TetR variants was assayed by DNA retardation. A synthetic 42 bp DNA fragment carrying *tetO* was incubated with increasing amounts of the TetR variants and complex formation was analyzed by PAGE. All TetR variants show apparent operator affinities similar to that of wild-type TetR (not shown). The same analysis was done with the spin-labeled TetR variants. The results are shown in Figure 2(a). The modification leads to reduced operator binding of TetR N47C. The close proximity of this position to the recognition helix α3 (positions 28-44) could lead to interference of the MTS spin label with operator DNA. However, a sample taken after the 170 K electron paramagnetic resonance (EPR) measurement showed complete binding of the modified TetR to DNA under the conditions of spectroscopy as analyzed by PAGE (see Figure 2(b)). All other spin-labeled TetR variants bind *tetO* as wild-type or better. These results extend the respective *in vivo* observations, since they demonstrate that the amino acid exchanges to cysteine and the attachment of the

Table 1. Average interspin distances in solution and C$^\beta$ distances from the crystal structure of TetR-([Mg-tc]$^+$)$_2$

		Distance (nm)[a]					
		I22C I22C′	N47C N47C′	R128C′ D180C	T152C Q175C	A161C Q175C	T202C T202C′
TetR tc	(C$^\beta$-C$^\beta$)[b]	1.18	2.9	1.12	1.60	1.2[c]	1.76
TetR tc		<1.0	2.0	1.2	1.7	1.6	1.7
TetR	(C$^\beta$-C$^\beta$)[d]	1.33	2.86	1.08			1.76
TetR		1.6	1.2-1.5	1.8	1.6	1.7	1.8
TetR *tetO*	(C$^\beta$-C$^\beta$)[e]	2.1	2.1				
TetR *tetO*		1.5	1.2-1.5	1.7	1.6	1.5	1.8

The distance distribution width for all samples was in the range from 0.45 to 0.65 nm.

[a] The standard error as calculated from the difference between simulated and experimental spectra is less than 10 %.

[b] The distances were determined from the 2.3 Å resolution crystal structure of the induced Tet repressor (Hinrichs *et al.*, 1994).

[c] The loop segment between 156 and 164 is not resolved in the crystal structure. The distances between the amino acid residues 161 and 175 were estimated using a modeled loop segment.

[d] The distances were determined from the 2.4 Å resolution crystal structure of the inducer free Tet repressor (Orth *et al.*, 1998). The loop segment between 151 and 164 is not resolved in this structure.

[e] The distances were determined from a model of the DNA reading heads of TetR adapted to fit on *B*-form DNA.

Table 2. *In vivo* repression and induction by tc

	β-Galactosidase activity (%)	
	pWH624 derivative	
tetR variant	No tc	0.4 μM tc
Wild-type	0.0 ± 0.2	100.0 ± 5.1
I22C	0.05 ± 0.1	94.5 ± 1.9
N47C	0.05 ± 0.05	92.4 ± 3.9
T152C/Q175C	0.1 ± 0.1	96.2 ± 1.5
A161C/Q175C	0.0 ± 0.1	99.2 ± 2.5
R128C′/D180C	0.1 ± 0.2	91.7 ± 2.1
T202C	0.01 ± 0.1	92.0 ± 1.5

The host strain was WH207pWH1012 transformed with pWH624 variants. β-Galactosidase activities are given in Miller units (Miller, 1972). Expression in the absence of *tetR* was set to 100% and corresponds to 235(±12) units. TetR wild-type represses the activity to 0.02 unit. The final concentration of tc was 0.4 μM for the overnight and log cultures.

spin label do not (at position 47 only marginally) affect operator binding *in vitro*.

The equilibrium association constants $K_{\alpha=1}$ of tc binding to the TetR variants and their spin-labeled modifications were determined as described (Takahashi *et al.*, 1986). The results are displayed in Table 3. All TetR variants show affinity for tc similar to that of wild-type and the modification with MTS spin label has no significant influence on binding of tc.

Taken together, all TetR mutants show wild-type activities *in vivo*, similar and saturating *in vitro* operator and inducer binding, and the modification of the cysteine residues by MTS spin label has no, or only little, influence on the *in vitro* activities. Thus, the correlation of the EPR spectra with different conformational states of TetR is possible.

Determination of conformational changes by EPR spectroscopy

The spin-spin interaction between two spin labels attached to a protein is composed of static dipolar interaction, modulation of the dipolar interaction by the residual motion of the spin-label side-chains and exchange interaction. The static dipolar interaction leads to a broadening of the spectrum if the interspin distance is less than 2.5 nm. Absolute values of the interspin distance have been calculated from a detailed line shape analysis of spectra measured below 200 K (Steinhoff *et al.*, 1991, 1997; Rabenstein & Shin, 1995; Thorgeirsson *et al.*, 1997). The modulation of the dipolar interaction due to the residual motion of the spin labels at room temperature allows an estimation of the inter-residue distances below 2.0 nm (Mchaourab *et al.*, 1997). The exchange interaction requires partial overlap of the nitrogen π-orbitals of the two interacting nitroxide groups and leads to a significant line broadening for distances of less than 1.0 nm (Closs *et al.*, 1992; Fiori & Millhauser, 1995).

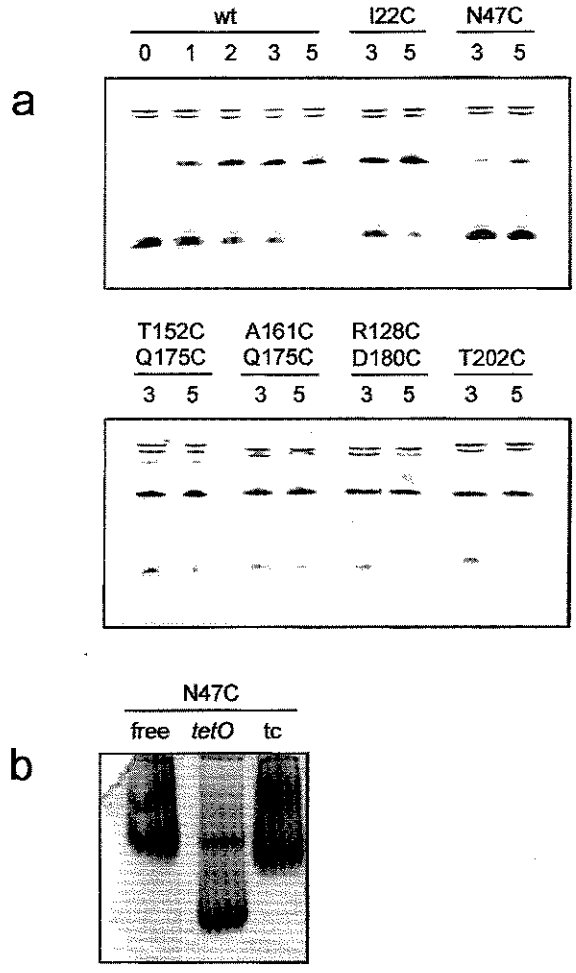

Figure 2. Operator binding of spin-labeled TetR variants analyzed by DNA and protein mobility shift. (a) DNA retardation on 10% PAGE are shown for wild-type and all spin-labeled TetR variants as indicated on the top of each gel: 2.5 pmol of operator DNA (*tetO*) was incubated with different amounts of spin-labeled TetR. The leftmost five lanes of the upper photograph show the analysis with 0/2.5/5/7.5/12.5 pmol of wild-type TetR, which had undergone the spin-labeling reaction, followed by 7.5/12.5 pmol for each spin-labeled TetR variant. The numbers on the top of the gel indicate the molar ratio of TetR to *tetO*. (b) The mobility of free, tc-bound and operator-bound forms of spin-labeled TetR N47C was analyzed by native 10% PAGE. Aliquots of the spin-labeled proteins were analyzed directly after recording the EPR spectra.

Table 3. Equilibrium association constants $K_{\alpha=1}$ of TetR variants and spin-labeled TetR variants with tc

TetR variant	$K_{\alpha=1}$ ($M^{-1} \times 10^9$)	+MTSSL $K_{\alpha=1}$ ($M^{-1} \times 10^9$)
Wild-type	2.1 ± 0.5	4.0 ± 0.4
I22C	2.8 ± 0.5	2.6 ± 0.3
N47C	2.2 ± 0.6	5.8 ± 0.3
T152C/Q175C	4.3 ± 0.2	1.6 ± 0.2
A161C/Q175C	5.6 ± 0.2	2.3 ± 0.3
R128C′/D180C	2.2 ± 3.0	2.5 ± 0.2
T202C	2.2 ± 0.5	4.1 ± 0.4

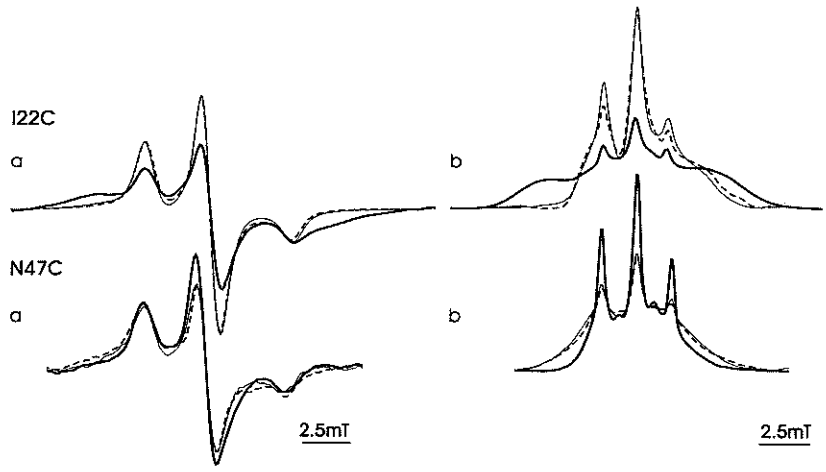

Figure 3. EPR spectra of spin-labeled TetR I22C and TetR N47C. First derivative absorption EPR spectra determined at (a) 170 K and (b) absorption spectra measured at room temperature of free (thin lines), DNA-bound (broken lines) and tc-bound (thick lines) proteins are shown. The spectra are normalized to equal spin number. The three narrow lines visible in the room-temperature spectra are attributed to small amounts of free label (2% in the case of I22C and 8% for N47C).

EPR spectra of free, operator-bound and tc-bound spin-labeled TetR variants were measured at 170 K in frozen solution to exclude dynamic effects and motional averaging of the dipolar broadening. Room temperature measurements ($T = 293$ K) were performed to characterize the side-chain mobility of the spin label and to reveal modulation of the dipolar interaction. The EPR spectra were normalized to represent the same number of spins. The results shown in Figures 3–5 reveal differences between the EPR spectral line shapes of the tc-bound, DNA-bound and free states of TetR of different degrees. To obtain a reference spectrum without spin-spin interaction between the spin labels, we constructed the mutant TetR N18C with a distance between the C^{β} atoms of 3.2 nm based on the crystal structure. The nitroxide groups of the spin labels attached to these residues cannot get closer than ~3.5 nm due to steric restrictions. Thus, line broadening due to dipolar interaction is much less than the natural line-

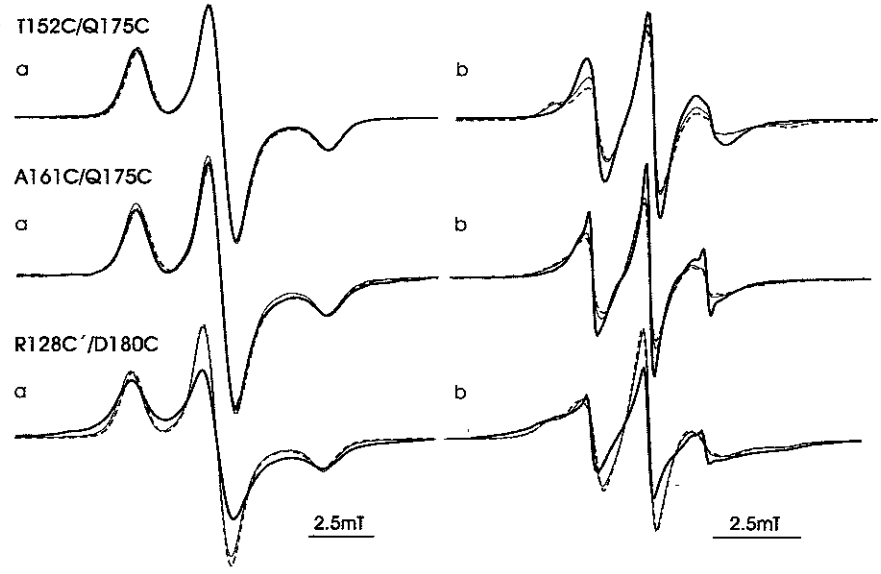

Figure 4. EPR spectra of spin-labeled TetR T152C/Q175C (p1), TetR A161C/Q175C (p2) and TetR R128C′/D180C (p3). First derivative absorption EPR spectra at (a) 170 K and (b) at room temperature of free (thin lines), DNA-bound (broken lines) and tc-bound (thick lines) proteins are shown. The spectra are normalized to equal spin number. The small narrow lines visible in the high-field region of the spectra of the tc-bound A161C/Q175C and R128C/D180C reveal unbound spin label, the relative concentration of which amounts to less than 1%. No free spin label is observable for T152C/Q175C.

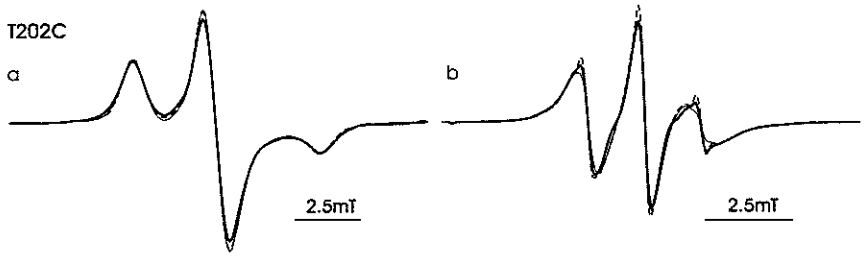

Figure 5. EPR spectra of spin-labeled TetR T202C. First derivative absorption EPR spectra at (a) 170 K and (b) at room temperature of free, DNA-bound and tc-bound proteins are shown. Spectra of the free proteins are shown as thin lines, spectra of tc-bound proteins as thick lines and those of DNA-bound proteins as broken lines. The spectra are normalized to equal spin number.

width. The respective spectrum is shown in Figure 6.

Additional information concerning the protein structure and structural changes can be obtained from the analysis of the spin label motion. The rotational isomerization of a spin label side-chain about internal bonds is modulated by van der Waals interactions of the nitroxide group with neighboring side-chain or backbone atoms. A spin label side-chain with the nitroxide group extending into the solvent is subject to little motional restriction relative to one located in the protein interior. Thus, conformational changes affecting the extent of tertiary interaction of the nitroxide group alter its mobility. Information on the spin label dynamics can be extracted from the EPR lineshape. A thorough analysis by means of spectra simulations (Freed, 1976; Steinhoff & Hubbell, 1996) revealed that the resonance position of the low-field and high-field extremes are a valuable measure of the nitroxide group mobility. For example, an outward shift of these extremes upon a conformational change is reliable evidence for an increase of the motional constraints. Isotropic dipolar coupling increases the line-widths at room temperature and can thus be separated from changes of the spin label dynamics (Mchaourab *et al.*, 1997). The shapes of the room-temperature spectra displayed in Figures 3-5 are discussed below in terms of these parameters.

Quantification of conformational changes by determination of interspin distances

To characterize the nature of the structural changes in TetR, powder spectra simulations were performed to estimate absolute values for the interspin distances. The parameters that describe the EPR spectrum in the absence of any spin-spin interaction were derived from the fitting of a simulated powder spectrum to the experimental data of TetR N18C. Figure 6 shows the identity of experimental and simulated spectra. The final values of the fitted g and A tensors are $g_{xx} = 2.0089$, $g_{yy} = 2.0065$, $g_{zz} = 2.0026$, $A_{xx} = 5.4$ G, $A_{yy} = 4.9$ G and $A_{zz} = 36.5$ G. The calculated powder spectrum was convoluted with a field-independent, line-shape function, composed of a superposition of 53 % Lorentian and 47 % Gaussian of 4.8 G and 4.1 G width, respectively. The fitted

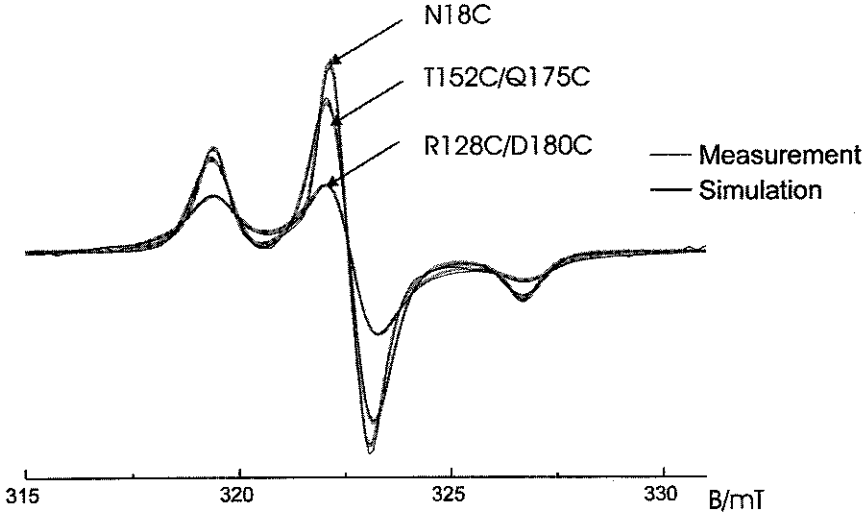

Figure 6. Comparison of measured and simulated EPR spectra of spin-labeled TetR variants. EPR spectra of the spin-labeled TetR N18C, T152C/Q175C, R128C'/D180C (thin lines) and simulated spectra (heavy lines) are shown. The spectra are normalized to equal spin number.

parameters are identical with those found for the MTS spin label attached to other proteins in a similar environment (Farahbakhsh *et al.*, 1995).

The experimental spectra are generally composed of species with different relative nitroxide orientations and interspin distances because of the flexibility of the spin label side-chains and the variety of conformational substates of the proteins in frozen solution. A fitting of simulated EPR spectra to the experimental data (Steinhoff *et al.*, 1997) with the assumption of a Gaussian interspin distance distribution yields the average interspin distance, d, and the distance distribution width, σ. The introduction of σ accounts for small amounts of singly spin-labeled proteins. Simulated powder spectra were calculated, and the values of d and σ were fitted to yield agreement between simulation and experiment. The g and A tensor values and the line-width parameters were held fixed at the values found for N18C. Examples of simulated and experimental spectra with interspin distances of 12(±1) nm (TetR R128C′/D180C) and 16(±1) nm (TetR T152C/Q175C) are displayed in Figure 6 in comparison to the spectra of TetR N18C. Again, simulated and experimental data agree well. The spectrum of the tc-induced conformation of TetR I22C/I22C′ is the only exception to the general agreement between experimental and calculated spectra. The spectral shape of the low-field and high-field regions of this sample could not be satisfactorily simulated (not shown). The best fit yields an interspin distance of 1.0 nm. Exchange interaction cannot be excluded in this distance range, which may be the reason for the poor fit. Thus, the obtained value of d represents an upper limit for this sample.

The calculated values of the interspin distances of all samples are summarized in Table 1. It should be noted that distances concluded from EPR measurements are between the spins, whereas distances taken from the crystal structure of TetR are between the C^{β} atoms. The maximum distance between the nitroxide group of the spin label side-chain and the respective C^{β} is about 0.6 nm. In the case of I22C/I22C′ and N47C/N47C′ the spin labels are attached to cysteine residues that face each other (cf. Figure 7). Consequently, the distances found between the NO moieties should be less than those between the respective C^{β} atoms. Agreement between interspin distances and C^{β} distances is revealed for the other spin-labeled positions of the induced protein. Thus, the interspin distance values given in Table 1 are reasonable as derived from the comparison with the distances between the respective C^{β}, the possible orientations of the spin labels with respect to each other, and the length of the nitroxide side-chain. The interspin distances obtained for the free, tc-bound or operator-bound states support the qualitative conclusion of conformational differences of TetR in its functional states. This is discussed in detail below.

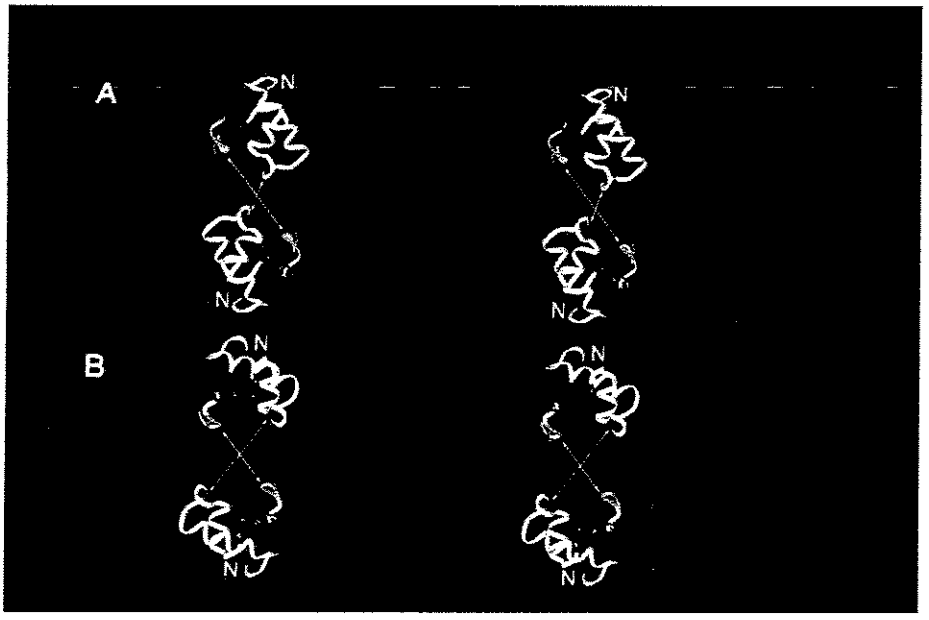

Figure 7. Stereo view of the possible location of DNA reading heads in operator-bound and tc-bound TetR. The DNA reading heads of the crystal structure of the TetR-($[Mg\text{-}tc]^{+}$)$_2$ complex (a) in comparison with a model of the DNA reading heads of TetR adapted to fit on *B*-form DNA (b) (DNA is not present in the Figure) are shown. The backbones are shown as gray ribbons, the recognition helices are colored in red. The engineered cysteine residues I22C and N47C are depicted in green and blue, respectively. The arrows connect residues for which interspin distance measurements were performed.

Ligand-dependent conformational differences of the DNA reading heads

The low-temperature EPR spectra of spin-labeled TetR I22C/I22C′ (Figure 3) exhibit a dipolar broadened line-shape for all three forms of the protein. The dipolar interaction in the DNA-bound repressor slightly exceeds that of the free protein. The strongest interaction is observed for the tc-bound form of TetR, where the spectral splitting is largely increased. The average interspin distances estimated from the fit of simulated to experimental spectra is less than 1.0 nm for tc-bound TetR, whereas 1.5 nm for the operator-bound and 1.6 nm for the free protein are calculated (Table 1). Thus, a distance change of more than 0.5 nm must occur in this region upon switching between tc-bound and operator-bound states. This conformational change is also reflected in the corresponding room temperature spectra. Large broadening due to spin-spin interaction leads to small amplitudes of the EPR signal of the protein-bound nitroxide groups. Thus, small amounts of free spin label, which is less than 2% in the present samples, dominates the first derivative spectral shape. We therefore show the integrated spectra in Figure 3(b). Extreme line broadening is revealed for tc-bound TetR. This must be due to spin-spin interaction, suggesting that the nitroxide moieties are nearly in van der Waals contact.

The spectra of TetR N47C/N47C′ reveal considerable spin-spin interaction and large changes between the DNA-bound and tc-bound forms (Figure 3). The binding of tc leads to a decrease of the line-width and consequently to an increased spectral amplitude, which is consistent with a decrease of the spin-spin interaction compared to the free protein. Fits of the spectra of the free and operator-bound proteins yield interspin distances between 1.2 and 1.5 nm, while that of the tc-bound form is increased to more than 2.0 nm. The influence of dipolar interaction on the spectra of the DNA-bound and free proteins is also seen in the room-temperature spectra. Both forms show significant line broadening in the low-field and high-field regions compared to the tc-bound form.

The distances between the spin labels differ in dependence on the bound ligand. They clearly define at least two different conformations of the DNA reading heads in the tc-bound or DNA-bound and free proteins. The binding of tc results in a decrease of the distances between positions 22 and 22′ of more than 0.5 nm, while an increase of the distance between positions 47 and 47′ of similar extent is found compared to the operator-bound form. These opposite effects are consistent with a twisting motion of the DNA reading heads with respect to each other. Such movements of the DNA reading heads of TetR have been formerly proposed for the induction process (Müller *et al.*, 1995). Rotating the DNA reading heads with respect to each other and a movement towards each other to shorten their distance by 0.5 nm are required to allow binding to two adjacent major grooves of *B*-form DNA. Figure 7 shows a possible model of the DNA reading heads of TetR bound to *B*-form DNA in comparison with the DNA reading heads according to the crystal data of the induced complex.

The EPR results reveal a distinct conformation of the DNA reading heads for the free protein. Indeed, the free protein and its DNA-bound conformation show very similar structure at the positions investigated. In contrast, the crystallographic data exhibit only a minor displacement of the DNA reading heads of the free compared to the induced protein (Orth *et al.*, 1998). According to the crystallographic data, the changes of the C^{β} distances between residues I22C and I22C′ and between residues N47C and N47C′ are less than 0.2 nm. The EPR data yield distance changes of more than 0.5 nm for both residue pairs. Since neighboring TetR dimers are arranged head-to-head in the crystal lattice, it is possible that intermolecular contacts that are absent in solution influence the positions of the DNA reading heads (Orth *et al.*, 1998).

Regions in the TetR core involved in structural changes

The low-temperature spectra of TetR T152C/Q175C and TetR A161C/Q175C (Figure 4) reveal only small contributions from spin-spin interactions. The simulated interspin distances for the three conformations are similar within a margin of 0.2 nm. However, the shapes of the room-temperature spectra of the three forms differ significantly. The low-field and high-field lines of the spectra of free and DNA-bound T152C/Q175C are composed of two components corresponding to distinct motional restrictions of the spin labels. Upon tc-binding, the spectral component of the more immobile fraction disappears and the spectral component that represents the mobile fraction increases. Since the immobile component does not occur in the spectra of the double mutant A161C/Q175C (see Figure 4), it most likely arises from the spin label attached to T152C. Thus, operator binding leads to structural changes in the vicinity of position 152 that restrict the residual motion of the attached label. The opposite is true for the tc-bound conformation, where the mobility of the spin label is increased and becomes indistinguishable from that of position 175.

A slight decrease of the line-width is detected for the room-temperature spectra of the tc-bound TetR A161C/Q175C compared to that of the free or operator-bound forms. This is indicated by the different shapes of the spectra in the low-field and high-field regions, and by the different amplitudes of the center peaks. Since the amplitude ratios of the three hyperfine lines are identical for the three conformations, the spectral changes are not caused by mobility changes of the spin label. They are most likely due to altered spin-spin interaction. The

observed behavior suggests an increase of the distance between positions 161 and 175 upon tc binding.

The low-temperature spectra of the free and operator-bound TetR R128C′/D180C (Figure 4) are nearly indistinguishable and show only weak contributions of dipolar broadening. However, strong interaction between the spin labels is detectable in the tc-bound form, as concluded from the increased line-width. Estimation of the interspin distances yields 1.2 nm for the tc-bound protein, whereas we find 1.7 nm for the DNA-bound and 1.8 nm for the free protein. The shapes of the room-temperature spectra support this finding. The spectra of the free and operator-bound TetR are very similar, whereas considerable line broadening is measured for tc-bound TetR. The excellent agreement of the distances derived from EPR spectroscopy and the crystal structure of the tc-bound protein is remarkable.

In summary, spectral differences between the tc-bound, DNA-bound and the free forms are detectable for all three investigated TetR mutants. Thus, different conformations of the variable loop and of α-helix 9 must exist. Intense interaction is observed between the positions 128 and 180 after tc binding, which is not detectable in the DNA-bound form. The results demonstrate that the C-terminal end of α-helix 9 must move away by 0.5 nm relative to position 128 upon DNA binding. Such a large movement must result in a shift of α-helix 9 and would bring the residues at positions 161 and 175 closer together. This is in agreement with the room-temperature spectra of TetR A161C/Q175C, where interactions between positions 161 and 175 are observed only in the DNA-bound form. A movement of α-helix 9 towards the variable loop away from the protein core could result in steric hindrance of the spin label bound at position 152, explaining the immobilization of the nitroxide group in the DNA-bound form.

These large conformational changes in the region of the variable loop and α-helix 9 during induction are in agreement with an induction model in which α-helix 9 locks the induced structure by closing the tc-binding pocket (Müller *et al.*, 1995). Furthermore, this would explain the previously noted need for great flexibility of this loop (Berens *et al.*, 1997).

The crystal structure of free TetR (Orth *et al.*, 1998) shows α-helix 9 to be displaced by 0.24 nm compared to the TetR-$([Mg\text{-}tc]^{+})_2$ structure. This is in agreement with the results presented here. However, the structural change as concluded from the EPR data may even be larger. The distances between residues R128 and D180 are similar for free TetR and the TetR-$([Mg\text{-}tc]^{+})_2$ complex in the crystal, whereas the EPR data yield a decrease of the interspin distance of more than 0.5 nm during induction. An alternative explanation of the observed distance shift could be a change of the spin label side-chain orientations. While this would also be evidence for a significant conformational change in the vicinity of residues R128C or D180C, it is unlikely to cause such a large interspin distance change. Thus, we conclude that the averaged solution structure of the respective region in free TetR is different from that of the crystal state.

Involvement of the dimerization surface in conformational changes

The drastic shift in the region of position 180 as discussed above cannot come about without influencing the position of the adjacent helices namely the α-helix 10. Spin labels bound at position 202 at the end of α-helix 10 are used as a detector of such alterations in the dimerization surface. In TetR T202C/T202C′ (Figure 5) the line width slightly increases upon tc binding, indicating a decrease of the distance between the C termini. The room-temperature spectra reveal similar mobilities for the spin labels in all three forms. The minor alterations in the dipolar interactions detected at this position in the three forms show that slightly different conformations must exist, implying that structural alterations of the four-helix bundle accompany the switch from one conformation to the other. This movement explains the large number of non-inducible mutants found at the dimer surface in former studies (Müller *et al.*, 1995).

Internal movements correlated to induction of Tet repressor

We have investigated three regions of TetR where conformational changes during induction have been proposed (Müller *et al.*, 1995). The data presented here define different structures for the DNA-bound and tc-bound proteins and imply that large structural changes influencing the entire protein must accompany the switch between these conformations. We suggest that the process of induction leads to a twisting motion of the DNA reading heads with respect to each other. Furthermore, our results directly demonstrate conformational changes in the region of α-helix 9 in the range of 0.5 nm during the process of induction, and also somewhat smaller movements within the four-helix bundle. Furthermore, the free TetR assumes a structure close to the DNA-bound form at the DNA reading heads and the tc-binding pocket.

Materials and Methods

Material and general methods

Chemicals of the highest purity available were obtained from Merck (Darmstadt, FRG), Serva (Heidelberg, FRG), Sigma (München, FRG), or Roth (Karlsruhe, FRG). The tc was purchased from Fluka (Buchs, CH). Enzymes for DNA restriction and modification were obtained from Boehringer Mannheim (Mannheim, FRG), New England Biolabs (Schwalbach, FRG), or Pharmacia (Freiburg, FRG). Oligonucleotides were obtained from

MWG Biotech (Munich, FRG) and MTS spin label from Reanal (Budapest, Hungary). Isolation and manipulation of DNA was done as described (Sambrook *et al.*, 1989). Sequencing was carried out according to the protocol provided by Pharmacia for use with phage T7 DNA polymerase with [α-^{32}P]dATP purchased from Amersham (Braunschweig, FRG).

Bacterial strains and plasmids

All bacterial strains are derived from *E. coli* K12. DH5α was used for general cloning, WH207 served for β-galactosidase assays and RB791 was used for overexpression of TetR variants. The plasmids pWH1012, pWH1201 and pWH624 were used for the determining TetR activity *in vivo* and the plasmid pWH1950D for overexpression of TetR variants (for references, see Berens *et al.*, 1997).

Construction of *tetR* mutants

Mutations were introduced into the cysteine-free TetR allele by PCR according to the three-primer method (Landt *et al.*, 1990). The conditions for PCR were chosen as described (Berens *et al.*, 1997). After mutagenesis, the entire *tetR* gene was sequenced to verify the desired and exclude secondary mutations. Seven different *tetR(D)* mutants bearing cysteine residues were constructed: Asn18 → Cys, denoted N18C; Ile22 → Cys, denoted I22C; Asn47 → Cys, denoted N47C; Thr202 → Cys, denoted T202C and the three double mutants Ala161 → Cys, Gln75 → Cys, denoted A161C/Q175C; Thr152 → Cys, Gln175 → Cys, denoted T152C/Q175C; Arg128 → Cys, Asp180 → Cys, denoted R128C/D180C. For construction of overexpressing plasmids, the respective pWH624 derivatives were digested with *Xba*I and *Sph*I, and the resulting 714 bp *tetR* fragments ligated into likewise digested pWH1950D to place the mutant *tetR* allele under *tac* promoter control.

β-Galactosidase assays

Repression and induction by tc were determined in *E. coli* WH207 pWH1012. The plasmid pWH1012 contains a *tetA-lacZ* transcriptional fusion. Cells were grown in LB supplemented with appropriate antibiotics at 28 °C. β-Galactosidase activities were determined as described (Miller, 1972). Three independent cultures were assayed for each mutant, and measurements were repeated at least twice.

Protein purification

E. coli RB791 transformed with pWH1950D derivatives was used for expression of TetR mutants. Purification of the proteins to homogeneity was done as described (Ettner *et al.*, 1996). Protein concentrations were determined by UV-spectroscopy using an extinction coefficient of $\varepsilon_{280} = 35{,}800\ M^{-1}\ cm^{-1}$ and by saturating titration with tc observing the change of fluorescence. Cysteine-containing TetR variants were stored in the presence of 5 mM DTT.

In vitro estimation of operator and tc-binding activities of TetR proteins

The binding activity of tc to Tet repressor was determined by tc and protein fluorescence using a Spex fluorimeter (Spex industries, Edison, NJ) equipped with double monochromators by measuring fluorescence emission of the drug at 515 nm and excitation at 370 nm as described (Takahashi *et al.*, 1986). Association constants $K_{\alpha=1}$ were determined at 28 °C. All measurements were repeated at least twice. The binding of Tet repressor to operator DNA was determined in DNA mobility shift analysis: 2.5-12.5 pmol of purified protein was incubated with 0.2 μg of non-specific DNA and 2.5 pmol of synthetic 42 bp DNA carrying *tet*-operator *tetO* in 20 mM Tris-HCl (pH 8.0), 5 mM $MgCl_2$, 40 mM KCl for ten minutes at ambient temperatures. The mobility of the DNA was analyzed by electrophoresis on 10% (w/v) polyacrylamide gels.

Spin-labeling of TetR variants

The proteins were dialyzed against 100 mM sodium phosphate buffer (pH 7.0) to dilute the concentration of DTT to 50 μM. A 100 μM protein solution was incubated with 1 mM spin label solution at 4 °C for 12 hours. The unbound spin label was removed by gel filtration using Sephadex G-25 mini columns from Pharmacia (Freiburg, FRG). Purified proteins were concentrated and treated in 20 mM Tris-HCl (pH 8.0), 5 mM $MgCl_2$, 40 mM KCl with a three fold excess of operator DNA or a tenfold excess of tc, respectively, to achieve the DNA-bound or tc-bound complexes.

EPR measurements and spectra simulations

EPR spectra were recorded using a home-made X-band EPR spectrometer equipped with an AEG H103 rectangular cavity or a Bruker dielectric cavity. The TetR samples were loaded into EPR quartz capillaries at a final concentration of 100 and 300 μM. A modified Oxford ESR 9 variable-temperature accessory was used for cooling of the samples to 170 K. Spectra were recorded with a modulation frequency of 52 kHz and a modulation amplitude of 1.5 G. The microwave power was varied between 100 μW and 2 mW depending on the sample type and temperature. After analog to 12 bit digital conversion, the data were processed in a PC. All measurements were repeated at least twice. The spin-labeled cysteine/TetR ratio was determined by double integration of the EPR spectra followed by comparison with standard solutions of MTS spin label and determination of the protein concentration. Interspin distances were calculated from the fit of simulated powder spectra according to the method by Steinhoff *et al.* (1997).

Acknowledgements

We thank Dr Veronika Helbl for modeling the DNA-bound reading heads. This work was supported by the Deutsche Forschungsgemeinschaft through SFB 394, SFB 473 and the Fonds der chemischen Industrie. B.T. was a recipient of a personal grant from the Boehringer Ingelheim Fonds.

References

Beck, C. F., Mutzel, R., Barbé, J. & Müller, W. (1982). A multifunctional gene (*tetR*) controls Tn*10*-encoded tetracycline resistance. *J. Bacteriol.* **150**, 633-642.

Berens, C., Schnappinger, D. & Hillen, W. (1997). The role of the variable region in Tet repressor for inducibility by tetracycline. *J. Biol. Chem.* **272**, 6936-6942.

Careaga, C. L. & Falke, J. J. (1992). Thermal motions of surface α-helices in the D-galactose chemosensory receptor. Detection by disulfide trapping. *J. Mol. Biol.* **226**, 1219-1235.

Closs, G. L., Forbes, M. D. E. & Piotrowiak, P. (1992). Spin and reaction dynamics in flexible polymethylene biradicals as studied by EPR, NMR, and optical spectroscopy and magnetic field effect. Measurements and mechanisms of scalar electron spin-spin coupling. *J. Am. Chem. Soc.* **114**, 3285-3294.

Cooper, A., McAlpine, A. & Stockley, P. G. (1994). Calorimetric studies of the energetics of protein-DNA interactions in the *E. coli* methionine repressor (MetJ) system. *FEBS Letters*, **348**, 41-45.

Ettner, N., Müller, G., Berens, C., Backes, H., Schnappinger, D., Schreppel, T., Pfleiderer, K. & Hillen, W. (1996). Fast large-scale purification of tetracycline repressor variants from overproducing *Escherichia coli* strains. *J. Chromatog. sect. A*, **742**, 95-105.

Farahbakhsh, Z. T., Huang, Q. L., Ding, L. L., Altenbach, C., Steinhoff, H. J., Horwitz, J. & Hubbell, W. L. (1995). Interaction of alpha-crystallin with spin-labeled peptides. *Biochemistry*, **34**, 509-516.

Farrens, D. L., Altenbach, C., Yang, K., Hubbell, W. L. & Khorona, H. G. (1996). Requirement of rigid-body motion of transmembrane helices for light activation of rhodopsin. *Science*, **274**, 768-770.

Fiori, W. R. & Millhauser, G. L. (1995). Exploring the peptide 3(10)-helix reversible alpha-helix equilibrium with double label electron spin resonance [published erratum appears in Biopolymers (1995) 37, 421]. *Biopolymers*, **37**, 243-250.

Freed, H. (1976). Theory of slow tumbling EPR spectra of nitroxides. In *Spin Labeling Theory and Applications* (Berliner, L. J., ed.), pp. 53-132, Academic Press, New York.

Gossen, M., Freundlieb, S., Bender, G., Müller, G., Hillen, W. & Bujard, H. (1995). Transcriptional activation by tetracyclines in mammalian cells. *Science*, **268**, 1766-1769.

Hansen, D., Altschmied, L. & Hillen, W. (1987). Engineered Tet repressor mutants with single tryptophan residues as fluorescent probes. Solvent accessibilities of DNA and inducer binding sites and interaction with tetracycline. *J. Biol. Chem.* **262**, 14030-14035.

Hecht, B., Müller, G. & Hillen, W. (1993). Noninducible Tet repressor mutations map from the operator binding motif to the C terminus. *J. Bacteriol.* **175**, 1206-1210.

Hillen, W. & Berens, C. (1994). Mechanisms underlying expression of Tn*10* encoded tetracycline resistance. *Annu. Rev. Microbiol.* **48**, 345-369.

Hinrichs, W., Kisker, C., Düvel, M., Müller, A., Tovar, K., Hillen, W. & Saenger, W. (1994). Structure of the Tet repressor-tetracycline complex and regulation of antibiotic resistance. *Science*, **264**, 418-420.

Hubbell, W. L. & Altenbach, C. (1994). Investigation of structure and dynamics in membrane proteins using site-directed spin labeling. *Curr. Opin. Struct. Biol.* **4**, 566-573.

Hubbell, W. L., Mchaourab, H. S., Altenbach, C. & Lietzow, M. A. (1996). Watching proteins move using site-directed spin labeling. *Structure*, **4**, 779-783.

Kisker, C., Hinrichs, W., Tovar, K., Hillen, W. & Saenger, W. (1995). The complex formed between Tet repressor and tetracycline-Mg^{2+} reveals mechanism of antibiotic resistance. *J. Mol. Biol.* **247**, 260-280.

Kolb, A., Busby, S., Buc, H., Garges, S. & Adhya, S. (1993). Transcriptional regulation by cAMP and its receptor protein. *Annu. Rev. Biochem.* **62**, 749-795.

Landt, O., Grunert, H. P. & Hahn, U. (1990). A general method for rapid site-directed mutagenesis using the polymerase chain reaction. *Gene*, **96**, 125-128.

Lee, G. F., Lebert, M. R., Lilly, A. A. & Hazelbauer, G. L. (1995). Transmembrane signaling characterized in bacterial chemoreceptors by using sulfhydryl cross-linking *in vivo*. *Proc. Natl Acad. Sci. USA*, **92**, 3391-3395.

Lewis, M., Chang, G., Horton, N. C., Kercher, M. A., Pace, H. C., Schumacher, M. A., Brennan, R. G. & Lu, P. (1996). Crystal structure of the lactose operon repressor and its complexes with DNA and inducer. *Science*, **271**, 1247-1254.

Mchaourab, H. S., Oh, K. J., Fang, C. J. & Hubbell, W. L. (1997). Conformation of T4 lysozyme in solution. Hinge-bending motion and the substrate-induced conformational transition studied by site-directed spin labeling. *Biochemistry*, **36**, 307-316.

Miller, J. H. (1972). *Experiments in Molecular Genetics*, Cold Spring Harbor Laboratory Press, Cold Spring Harbor, NY.

Müller, G., Hecht, B., Helbl, V., Hinrichs, W., Saenger, W. & Hillen, W. (1995). Characterization of non-inducible Tet repressor mutants suggests conformational changes necessary for induction. *Nature Struct. Biol.* **2**, 693-703.

Oesterhelt, D. (1998). Structure and mechanism of the family of retinal proteins from halophilic archaea. *Curr. Opin. Struct. Biol.* **8**, 489-500.

Orth, P., Cordes, F., Schnappinger, D., Hillen, W., Saenger, W. & Hinrichs, W. (1998). Conformational changes of the Tet repressor induced by tetracycline trapping. *J. Mol. Biol.* **279**, 439-447.

Perozo, E., Cortes, M. & Cuello, L. G. (1998). Three-dimensional architecture and gating mechanism of a K^+ channel studied by EPR spectroscopy. *Nature Struct. Biol.* **5**, 459-469.

Rabenstein, M. D. & Shin, Y. K. (1995). Determination of the distance between two spin labels attached to a macromolecule. *Proc. Natl Acad. Sci. USA*, **92**, 8239-8243.

Sambrook, J., Fritsch, E. F. & Maniatis, T. (1989). *Molecular Cloning: A Laboratory Manual*, Cold Spring Harbor Laboratory Press, Cold Spring Harbor, NY.

Steinhoff, H.-J. & Hubbell, W. L. (1996). Calculation of electron paramagnetic resonance spectra from Brownian dynamics trajectories: Application to nitroxide side chains in proteins. *Biophys. J.* **71**, 2201-2212.

Steinhoff, H. J., Dombrowsky, O., Karim, C. & Schneiderhan, C. (1991). Two dimensional diffusions of small molecules on protein surfaces: an EPR study of the restricted translational diffusion of protein bound spin labels. *Eur. Biophys. J.* **20**, 293-303.

Steinhoff, H.-J., Mollaaghababa, R., Altenbach, C., Hideg, K., Krebs, M., Khorana, H. G. & Hubbell, W. L. (1994). Time-resolved detection of structural changes during the photocycle of spin-labeled bacteriorhodopsin. *Science*, **266**, 105-107.

Steinhoff, H.-J., Mollaaghababa, R., Altenbach, C., Khorana, H. G. & Hubbell, W. L. (1995). Site

directed spin labeling studies of structure and dynamics in bacteriorhodopsin. *Biophys. Chem.* **56**, 89-94.

Steinhoff, H.-J., Radzwill, N., Thevis, W., Lenz, V., Brandenburg, D., Antson, A., Dodson, G. & Wollmer, A. (1997). Determination of interspin distances between spin labels attached to insulin: comparison of electron paramagnetic resonance data with the X-ray structure. *Biophys. J.* **73**, 3287-3298.

Takahashi, M., Altschmied, L. & Hillen, W. (1986). Kinetic and equilibrium characterization of the Tet repressor-tetracycline complex by fluorescence measurements. Evidence for divalent metal ion requirement and energy transfer. *J. Mol. Biol.* **187**, 341-348.

Thorgeirsson, T. E., Xiao, W., Brown, L. S., Needleman, R., Lanyi, J. K. & Shin, Y.-K. (1997). Transient channel-opening in bacteriorhodopsin: an EPR study. *J. Mol. Biol.* **273**, 951-957.

Tiebel, B., Aung-Hilbrich, L. M., Schnappinger, D. & Hillen, W. (1998). Conformational changes necessary for gene regulation by Tet repressor assayed by reversible disulfide bond formation. *EMBO J.* **17**, 5112-5119.

Zhang, R.-G., Joachimiak, A., Lawson, C. L., Schevitz, R. W., Otwinowski, Z. & Sigler, P. G. (1987). The crystal structure of *trp* aporepressor at 1.8 Å shows how binding tryptophan enhances DNA affinity. *Nature*, **327**, 591-597.

Edited by N. Baumeister

(Received 29 January 1999; received in revised form 6 May 1999; accepted 13 May 1999)